Propagation of surface sound in superfluid ^{3}He-^{4}He†

D. O. Edwards, S. Y. Shen,* J. R. Eckardt,‡ P. P. Fatouros, and F. M. Gasparini§
Department of Physics, The Ohio State University, Columbus, Ohio 43210
(Received 18, February 1975)

"Surface sound," a longitudinal compressional wave in ^{3}He adsorbed on the surface of superfluid ^{4}He, has been propagated in the temperature range from 20 to 120 mK. Measurements of the surface-sound velocity and of the surface tension are compared to a model of interacting surface ^{3}He quasiparticles. A least-squares fit to the model is used to obtain the ^{3}He binding energy, $\epsilon_0/k_B = 2.28 \pm 0.03$ K, the ^{3}He effective mass, $M/m_3 = 1.3 \pm 0.1$, and some limits on the sign and magnitude of the effective interaction between the quasiparticles. The interaction is found to be very weak and predominantly repulsive at large distances.

I. INTRODUCTION

There is considerable interest in studying the many-body properties of ^{3}He atoms adsorbed on the surface of superfluid helium, since this system is a very close approximation to a two-dimensional Fermi liquid, and one in which two-dimensional superfluidity might occur at sufficiently low temperatures.

The existence of ^{3}He quasiparticle states which are bound to the surface of superfluid ^{4}He was first proposed by Andreev[1] in order to explain the effect of ^{3}He on the surface tension. The surface states have energy[2]

$$\epsilon = -\epsilon_0 + p^2/2M , \tag{1}$$

where the momentum p is confined to the plane of the surface. One may view the adsorbed ^{3}He as a two-dimensional quasiparticle gas exerting a "pressure" which decreases the surface tension below the value for pure ^{4}He. In a recent experimental study of surface ^{3}He, Guo *et al.*[3] obtained approximate values for the binding energy ϵ_0 and the effective mass M by extensive measurements of the surface tension of dilute ^{3}He-^{4}He mixtures. In the present paper we describe an experiment on a hydrodynamic property of the surface, namely, the propagation of "surface sound"[4] which, in the range of temperature and concentration that we have investigated, is just an adiabatic compressional wave in the two-dimensional gas of surface ^{3}He. From the velocity of surface sound one obtains information about the inertial mass density and the adiabatic compressibility of the two-dimensional system. From the latter it is possible, in principle, to derive the sign and magnitude of the surface ^{3}He-^{3}He interaction.

The phenomenological theory of surface sound has been developed by Andreev and Kompaneets,[4] who called it "surface second sound," and who were the first to propose its existence. In their theory the behavior of the surface and of the adsorbed ^{3}He is described by a set of two-dimensional two-fluid hydrodynamic equations which are closely analogous to the three-dimensional equations for the bulk of the liquid. The normal fluid on the surface is composed of surface excitations which are quantized capillary waves (ripplons) and adsorbed ^{3}He quasiparticles. On solving the equations for small-amplitude oscillations, Andreev and Kompaneets found, in addition to the already known capillary waves, a form of longitudinal wave in the surface of the helium (surface sound) in which no vertical displacement takes place. The surface sound has velocity u_s given by

$$\nu_n u_s^2 = -\left(\frac{\partial \sigma}{\partial \ln N_s}\right)_{S/N_s} , \tag{2}$$

where ν_n is the mass of the surface normal fluid per unit area, σ is the surface tension, $N_s = -(\partial\sigma/\partial\mu_3)_T$ is the number of surface ^{3}He per unit area, $S = -(\partial\sigma/\partial T)_{\mu_3}$ is the entropy per unit area, and μ_3 is the ^{3}He chemical potential. The normal-fluid mass ν_n includes contributions from both ripplons and surface ^{3}He. Andreev and Kompaneets's theory is based on the assumption that at low temperatures the dynamics of the liquid can be adequately described by two *noncoupled* Boltzmann equations for the bulk and the surface excitations.

We have measured the velocity of surface sound with a time-of-flight method in two samples of liquid with different, but very small ^{3}He concentrations. The ratio of the volume of the liquid to the area of the free surface accessible to ^{3}He was such that, below about 90 mK, all the ^{3}He was adsorbed on the surface and none was dissolved in the bulk liquid. We could therefore vary the temperature without changing the number density of ^{3}He on the surface. We have also measured the surface tension, using a capillary-rise method, in the same temperature range and between 90 and 300 mK,

where the ^{3}He dissolves into the interior of the liquid. The behavior of the surface tension above 100 mK is very sensitive to the value of the binding energy and we were able to obtain an accurate value of ϵ_0 from these data.

Our experiment shows that Eq. (2) accurately predicts the velocity of surface sound in the low-temperature region where coupling between the surface and the bulk excitations is small. We also find that the surface ^{3}He at low densities behaves as an almost ideal two-dimensional Fermi gas with very small or negligible effects from interactions between the quasiparticles. The surface-tension and surface-sound data have been used together to obtain accurate values for ϵ_0 and M and to give some limits on the magnitude and sign of the quasiparticle interaction. Part of the work has been briefly published in a Letter.[5]

II. EXPERIMENTAL METHODS

A. General

The principle of our technique is to generate surface sound by applying a heat pulse to a resistor intersecting the surface and to detect the signal with a bolometer intersecting the surface at a known distance from the heater. The velocity of sound is then determined from the time of flight. The surface number density N_s is obtained by combining the sound-velocity data with accurate simultaneous measurements of the surface tension and fitting all the data to the theoretical model.

Two concentrations of ^{3}He-^{4}He solution were studied. The first sample of 0.337 l of liquid was ordinary commercial helium and it contained about 0.13 ppm of ^{3}He. A measured small amount of ^{3}He corresponding to 0.0575 ppm was added to the first sample to form the second. The surface number densities for the two samples at 0 K were later found to be 0.97×10^{14} and 1.42×10^{14} cm^{-2}.

B. Experimental cell

The measurements were performed in a copper cell 9.5 cm in diameter and 17 cm in height cooled by a dilution refrigerator. The temperature was measured by an external cerium magnesium nitrate (CMN) magnetic thermometer[6] attached to the cell. The thermometer was made of CMN and silver nitrate crystals compressed around silver wires and encapsulated in an epoxy shell. It was calibrated against a Cryocal[7] germanium thermometer previously calibrated against the ^{3}He vapor-pressure scale. Errors in temperature are estimated to be less than 1%.

The cell was originally designed for the study[8] of scattering of low-energy helium atoms at the surface of liquid helium at low temperatures. The beam of helium atoms is produced by evaporating some of the superfluid film covering the surface of a graphite resistor with a heating pulse of ~20-μsec duration. A similar resistor acting as a bolometer is used to detect the beam. Three of these resistors can be moved by superconducting stepping motors[9] in a vertical circle of radius 4 cm whose center lies on the liquid surface. The surface sound was discovered accidentally when the transmitter and detector were allowed to intersect the surface of the liquid. The cell also contains three other stationary graphite resistors which intersect the liquid surface. Altogether there are seven transmitter-receiver pairs for the propagation of surface sound. Two sizes of resistors were used: 3.9×3.9 and 7.5×7.5 mm^2. They were prepared[10] from 500-Ω/square IRC resistance strips which consist of a thin graphite film on a plastic laminate. Conductive silver epoxy was used to bond leads to the graphite.

The upper part of the experimental cell contains a bundle of fine copper wires and the wall of the cell is lined with velvet to reduce reflections from the wall in the atomic-beam experiment. These materials together give an area of about 10 000 cm^2, which was covered with saturated helium film and which was accessible to surface ^{3}He.

C. Detection of surface sound

Figure 1 shows the receiver circuit for the detection of surface sound. The receiver is a graphite resistor R which is used as a bolometer and which is one arm of a Wheatstone bridge, another arm being the variable standard resistor S. The bridge is connected to a 125-kHz tuned amplifier in a positive-feedback oscillator circuit. The condition that the loop gain be unity maintains the resistance and hence the temperature of the receiver constant. When heat is incident on the receiver it causes a transient decrease in the oscillator power W_R which is used to measure the signal.

The voltage across R passes through an amplifier and then a squarer before going into a Biomation[11] 802 transient recorder which digitizes the analog signal. A sufficiently high signal-to-noise ratio is

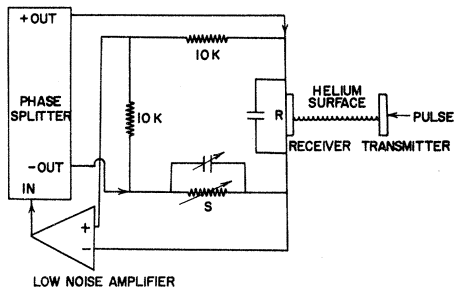

FIG. 1. Positive-feedback oscillator circuit used for the detection of surface sound at receiver R.

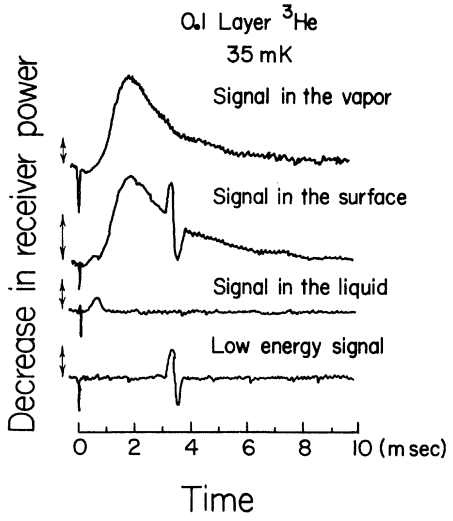

FIG. 2. Observation of surface sound. The upper signal was obtained with the pulsed element and the detecting element above the liquid surface, the second signal with elements intersecting the surface, and the third with both elements completely immersed. The signal in the vapor corresponds to a roughly Maxwellian distribution of atoms. The signal in the liquid arises from the ballistic propagation of phonons. The additional effect in the surface is the surface sound. The last signal is surface sound when the heat pulse applied to the heater is not large enough to generate atoms. The vertical arrow at the beginning of each signal represents a change of $\ln W$ in the power dissipated in the receiver circuit.

achieved by averaging over several thousand experiments using a Nicolet[12] 1072 multichannel signal averager.

The analysis of the dynamical behavior of the detector-bridge system is complicated but various tests have shown that the effective time constant in the configuration we used in this experiment is about 50 μsec.

D. Measurement of the surface tension

A gold-plated quartz capacitor[10] with an active area of 1.66×0.69 cm^2 and an average separation of 5.49×10^{-3} cm was used to determine the surface tension. The same apparatus has been used to measure the surface tension at the λ point[13] and the contribution from ripplons to the surface tension of pure ^{4}He.[14,15] The method makes use of a voltage V applied between the plates of the capacitor so as to keep the position of the meniscus constant. In this case the change in the square of the applied voltage, δV^2, required to counterbalance the effect of a change $\delta\sigma$ in the surface tension is proportional to $\delta\sigma$. Using the principle of virtual work,

$$\delta\sigma = -\frac{\epsilon-1}{8\pi}\frac{\delta V^2}{2t}, \tag{3}$$

where ϵ is the dielectric constant of helium and t is the separation of the capacitor plates at the meniscus. In deriving Eq. (3) we have ignored the effect of changes in the density of the liquid and the vapor, which are negligible at the temperatures in the present work. Equation (3) is correct regardless of whether the capacitor plates are truly parallel or even smooth as long as t is taken to be the separation of the plates at the meniscus of the liquid. Eckardt[15] has shown that the value of t at the level used in the present experiment is equal within $\pm1.6\%$ to the average plate separation obtained by measuring the empty capacitance, giving $t=(5.49\pm0.09)\times10^{-3}$ cm.

III. RESULTS AND DISCUSSION

A. Surface sound

Surface sound was first observed in the manner shown in Fig. 2. These measurements demonstrate quite conclusively that the surface-sound signal is propagated only in the surface of the liquid. (The data in Fig. 2 were obtained in an early experiment, reported in Ref. 16, where the number density of ^{3}He on the surface was known only approximately.)

Surface sound can also be generated by applying a heating pulse to a transmitter above the liquid. In this case the surface sound is generated by the evaporated helium atoms striking the surface. However, in all our measurements of the sound velocity the heater intersected the liquid surface.

A typical surface-sound signal consists of a heating of the receiver followed by a series of alternately cold and warm oscillations which decrease rapidly in amplitude as shown in Fig. 3. The beginning of the first peak was taken to indicate the arrival of the surface-sound wave from which the flight time was determined. The flight time could usually be determined to about 25 μsec.

Figure 3 shows some traces obtained from the signal averager when the heat pulse Q applied to the transmitter was varied. In these measurements the transmitter was of area 0.56 cm^2. When the input heat Q is above ~32 merg, as in the fourth trace, the effect of atoms generated by the part of the transmitter above the liquid surface can be observed. When the atomic signal is visible surface sound appears to arrive at an earlier time than when no atoms can be seen (see Fig. 4). This observation is consistent with the idea that the evaporated atoms striking the liquid surface can create a surface sound wave at a point closer to the receiver than the transmitter. Figure 4 shows that when small heat pulses below 32 merg are used, the measured flight time is independent of Q. We used heat inputs Q of 2.5–5 merg in our time-of-flight measurements of the velocity.

Figure 5 shows a check on the distances between the graphite transducers and of the response time

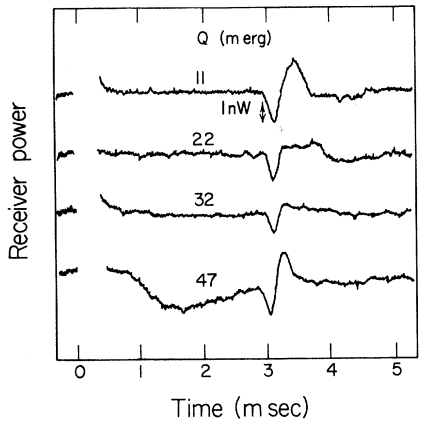

FIG. 3. Effect of heat input to the transmitter Q on the surface-sound time of flight. The traces were taken at 33 mK. The vertical axis in each trace is the power dissipated in the receiver circuit and the horizontal axis is time. The distance of propagation is 84 mm. The area of the transmitter was 0.56 cm^2. The decrease in the receiver power at a time of roughly 3 msec is due to the arrival of the surface sound. In the fourth trace the decrease in the receiver power which begins at about 1 msec is due to atoms evaporated from the transmitter. Note that the surface-sound signal arrives at an earlier time in the fourth trace than in the others.

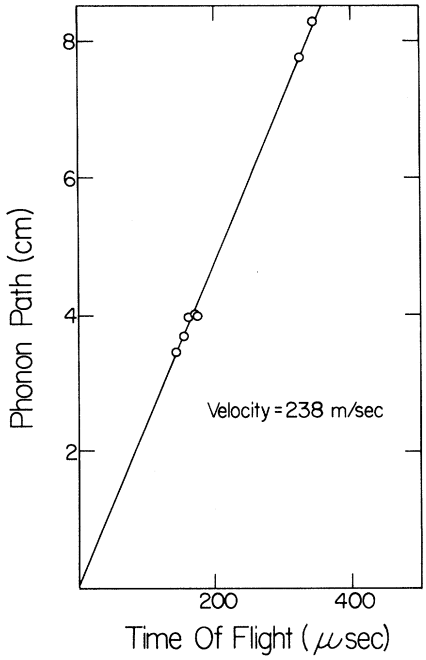

FIG. 5. Check of transmitter-receiver distances using phonons at 30 mK. Phonons were generated at the immersed portion of the transmitter by the application of a heat pulse. The same receiver circuit shown in Fig. 1 was used to detect the phonons.

of the receiver circuit. We measured the phonon velocity in the liquid using different distances of propagation. We obtain 238 ± 4 m/sec, in good agreement with the known value of the first-sound velocity.[17]

Figure 6 is a plot of the flight time of surface sound versus the distance traveled on the liquid surface. A straight line passing through the origin is obtained showing that the velocity of surface sound is independent of distance. The actual path lengths for the transmission of surface sound are longer than the geometrical distances because we have to take into account the profile of the liquid rising against the transmitter and the receiver due to surface tension.[10] This correction, which we have taken into account in Fig. 6, is $(\sqrt{2}-1)2(2\sigma/\rho g)^{1/2} = 0.604$ mm.

We investigated the effect on the surface sound of different power levels in the receiver circuit.

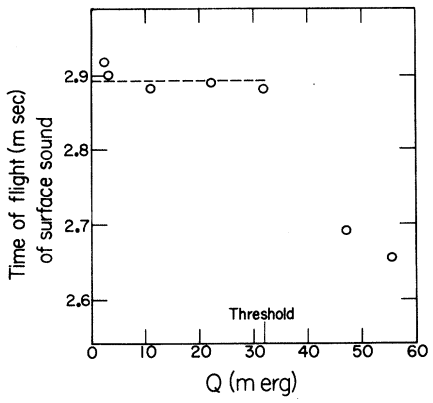

FIG. 4. Flight time at 33 mK for a distance of 84 mm and a transmitter of area 0.56 cm^2. When the heat applied to the transmitter Q is above the threshold value indicated, atoms evaporated from the transmitter generate surface sound which has a shorter flight time.

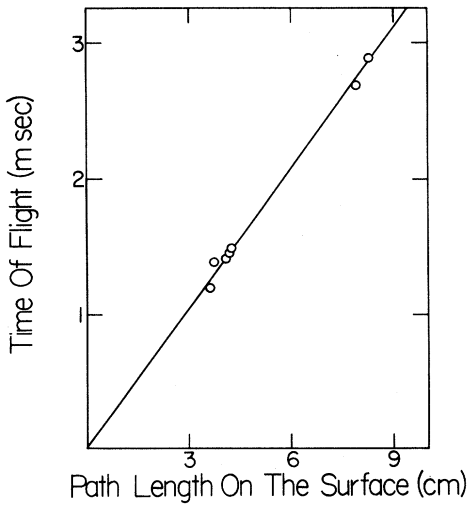

FIG. 6. Surface-sound time of flight versus path length at 41 mK (first sample).

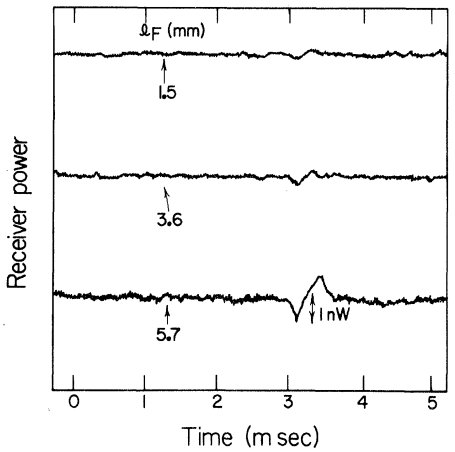

FIG. 7. Dependence of signal size on the length of the transmitter covered by saturated film, l_F (in mm), at 37 mK in the first sample of liquid.

It was found that the size of the surface-sound signal increases with the power dissipated in the receiver, W_R, but the velocity of surface sound remains constant, independent of W_R. A larger W_R corresponds to a higher receiver temperature and the increase in the strength of the signal is probably associated with a decrease in the time constant of the receiver circuit. In making the velocity measurements W_R was about 50 nW while the temperature of the receiver varied from 100 to 200 mK depending on the degree of immersion and on the bath temperature.

The size of the surface-sound signal was found to depend on the degree of immersion of the transmitter in the liquid. Figure 7 shows signals obtained when the transmitter was lifted out of the liquid in steps. The temperature of the receiver above the liquid was about the same for all three traces. The general observation is that the signal strength is roughly proportional to the length of the transmitter outside the liquid, which indicates that the saturated film covering the transmitter above the liquid meniscus plays a role in the generation of surface sound. The length of the superfluid film l_F on the transmitter in each case is indicated on the traces in Fig. 7. The mechanism for the generation of surface sound will be explored in relation to these results in Sec. IV C.

With the above observations we were able to measure the time of flight of surface-sound pulses over a known path length independent of transmitter and receiver conditions. The resulting surface-sound velocities for the two samples that we studied are shown as a function of temperature in Fig. 8. The qualitative behavior of u_s is very similar for the two concentrations. In the region below 90 mK, where the ^{3}He remains entirely on the surface, the velocity increases with the temperature roughly as T^2, and in the region above 90 mK, where the ^{3}He begins to dissolve into the interior of the liquid, u_s decreases with temperature. The magnitude of the surface-sound signal also decreases rapidly in this second region and we were unable to detect any signal above about 130 mK. In the region above 90 mK the hydrodynamics of the surface cannot be completely independent of the normal fluid in the bulk of the liquid, therefore the decrease in u_s and the disappearance of the surface-sound signal is most probably due to damping by the ^{3}He in the bulk.

B. Surface tension

The technique described in Sec. II D allowed us to measure the difference between the surface tension of our sample at any two different temperatures. In our determination of the surface tension as a function of temperature we have chosen the surface tension at 300 mK as a reference point, the experimentally determined quantity being the difference $\sigma(0.3) - \sigma(T)$. Measurements,[14,15] at higher temperatures have shown that Atkins's[18] theory, in which the temperature dependence of the surface tension of pure ^{4}He is attributed to the ripplon contribution to the surface free energy, is asymptotically correct at low temperatures and is very accurate at 0.3 K and below. In fitting the data to our theoretical model of surface ^{3}He, we calculated the pure-^{4}He contribution to the temperature dependence of the surface tension using Atkins's formula

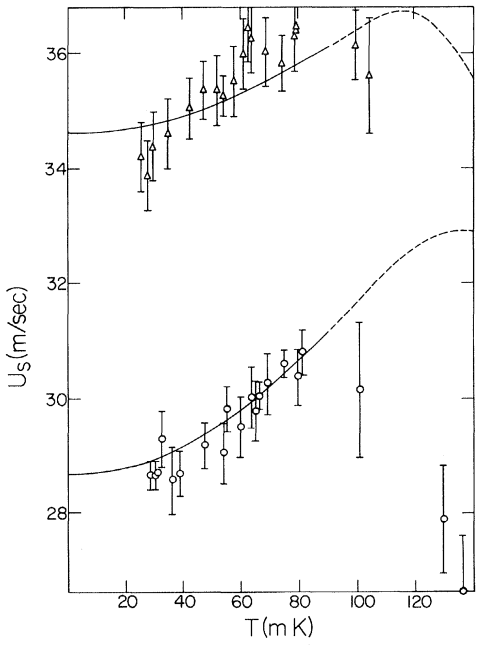

FIG. 8. Velocity of surface sound, u_s, as a function of temperature for the first sample (circles) and second sample (triangles). The curves, which are theoretical, are discussed in Sec. IV B.

$$\Delta\sigma_4 \equiv \sigma_4(T) - \sigma_4(0) = -(6.50\times10^{-3})T^{7/3} \text{ erg cm}^{-2} .$$

Also, the very small surface-tension depression due to ^{3}He at 300 mK was taken into account using the theoretical surface-^{3}He parameters (see Sec. IV B). As a result of this fit we were able to determine $\sigma_4(0) - \sigma(0.3)$ so as to display our results in absolute form as $\sigma_4(0) - \sigma(T)$.

The results of our measurements are shown in Fig. 9. The standard deviation is estimated to be about 0.01% of the total surface tension. The circles represent data on the first sample and triangles for the second. The dashed curve shows the temperature dependence of the surface tension of pure ^{4}He calculated from Atkins's theory. The solid curves are the theoretical fits to data on the two samples, which we will describe in Sec. IV B. The difference between the dashed curve and the data can be thought of as the "spreading pressure" of surface ^{3}He. For both samples below ~90 mK, the temperature-dependent part of the surface tension is approximately proportional to T^2, as we expect for a degenerate Fermi system. As the temperature increases above ~90 mK the ^{3}He dissolves and the surface tension rises rapidly and merges with the ^{4}He surface tension.

We observe that the temperature at which the surface ^{3}He begins to dissolve is lower for the higher (second) concentration. That is easily understood since the ^{3}He has a higher Fermi energy in the more concentrated sample and therefore begins to dissolve at a lower temperature. As we will show in Sec. IV B, the data in the dissolving region permit us to evaluate ϵ_0, the binding energy of ^{3}He to the surface, very accurately.

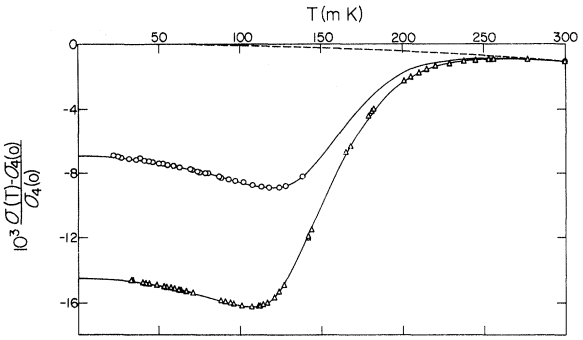

FIG. 9. Fractional change in surface tension from the value of pure ^{4}He at 0 K, $\sigma_4(0)$, as a function of temperature for the first sample (circles) and the second sample (triangles). The dashed line is the Atkins theory for pure ^{4}He. The solid curves are theoretical, fitted to the data as described in Sec. IV B.

IV. THEORY AND DISCUSSION

A. Theory of interacting surface quasiparticles

A general quasiparticle theory which we can use to compare with the properties of surface ^{3}He at low number densities [i.e., less than one atomic layer ($\sim 6\times10^{14}$ cm^{-2})] is similar to the analogous three-dimensional theory for dilute bulk solutions of ^{3}He in ^{4}He. Following the procedure described in Ref. 19, one can regard the quasiparticle energy spectrum as an expansion in the momentum squared:

$$\epsilon(\vec{p}) = -\epsilon_0 + p^2/2M + \gamma(p^4/2M) . \quad (4)$$

We also introduce a "forward scattering amplitude" $U_{\sigma\sigma'}(\vec{p}, \vec{p}')$ so that the change in the energy per unit area of the surface due to ^{3}He can be expanded up to second order in the quasiparticle distribution function $n_\sigma(\vec{p})$:

$$U^s = U_4^s + \sum_\sigma \int d\tau\, \epsilon(\vec{p}) n_\sigma(\vec{p}) + \frac{1}{2}\sum_\sigma \sum_{\sigma'} \int d\tau\, d\tau'\, U_{\sigma\sigma'}(\vec{p}, \vec{p}') n_\sigma(\vec{p}) n_{\sigma'}(\vec{p}') , \quad (5)$$

where $d\tau = d^2p/h^2$ and U_4^s is the energy of the pure-^{4}He surface. The amplitude $U_{\sigma\sigma'}$ is related to the Bardeen-Baym-Pines (BBP)-type interaction potential $V(\vec{p}, \vec{p}', \vec{q})$:

$$U_{\sigma\sigma'}(\vec{p}, \vec{p}') = [V^s(\vec{p}, \vec{p}', 0) - \delta_{\sigma\sigma'} V^s(\vec{p}, \vec{p}', \vec{p}' - \vec{p})] . \quad (6)$$

If the Fourier transform exists, then

$$V^s(\vec{p}, \vec{p}', \vec{q}) = \int d^2r\, e^{-i\vec{q}\cdot\vec{r}/\hbar} V^s(\vec{p}, \vec{p}', \vec{r}) , \quad (7)$$

where $V^s(\vec{p}, \vec{p}', \vec{r})$ is the interaction in real space. Even if the Fourier transform does not exist, Eqs. (5) and (6) may still be used, [19] but the interpretation of $V^s(\vec{p}, \vec{p}', \vec{q})$ must be modified. Expanding $V^s(\vec{p}, \vec{p}', \vec{q})$ up to quadratic terms,

$$V^s(\vec{p}, \vec{p}', \vec{q}) = V_0^s + \alpha_1(\vec{p} - \vec{p}')^2 + \alpha_2 \vec{p}\cdot\vec{p}' + \beta q^2 , \quad (8)$$

and using Eq. (6) one finds that the average value of $U_{\sigma\sigma'}(\vec{p}, \vec{p}')$ over all spin coordinates is

$$U(\vec{p}, \vec{p}') = \tfrac{1}{2}[V_0^s + (\alpha_1 - \beta)(\vec{p}' - \vec{p})^2 + \alpha_2(\vec{p}\cdot\vec{p}')] . \quad (9)$$

A slightly different approach and notation is that of Disatnik and Brucker, [20] who, in the analogous three-dimensional problem, expand $U(\vec{p}, \vec{p}')$ directly:

$$U(\vec{p}, \vec{p}') = v_0 + v_1(\vec{p}' - \vec{p})^2 + v_2\vec{p}\cdot\vec{p}' , \quad (10)$$

so that, in terms of our previous parameters,

$$v_0 = \tfrac{1}{2} V_0^s , \quad v_1 = \tfrac{1}{2}(\alpha_1 - \beta) , \quad v_2 = \tfrac{1}{2}\alpha_2 . \quad (11)$$

One should note that we have entirely neglected any interaction between the surface ^{3}He and the bulk quasiparticles so that the above theory is limited to the temperature and concentration range where the effect of dissolved ^{3}He can be neglected. Presumably the interaction with the bulk could be accounted for by introducing a further scattering amplitude between surface and bulk ^{3}He.

The expressions for the chemical potential μ_3, the surface tension σ, and the surface normal mass

density ν_n in this general model are given as functions of N_s and T in the Appendix. The surface entropy S can be obtained from these quantities using the thermodynamic relation

$$-S=\left(\frac{\partial\sigma}{\partial T}\right)_{\mu_3}=\left(\frac{\partial\sigma}{\partial T}\right)_{N_s}+N_s\left(\frac{\partial\mu_3}{\partial T}\right)_{N_s} \tag{12}$$

and the surface-sound velocity u_s is given by Eq. (2),

$$\nu_n u_s^2=-\left(\frac{\partial\sigma}{\partial\ln N_s}\right)_{S/N_s} . \tag{2}$$

We can restrict the number of adjustable parameters in the theory in the BBP[21] manner by neglecting the dependence of $V^s(\vec{p},\vec{p}',\vec{q})$ on $\vec{p}$ and $\vec{p}'$ and also dropping the term in γp^4 in the quasiparticle energy. Then α_1, α_2, and γ are all equal to zero. In most of the comparison between the experiment and theory to be described in Sec. IV B, we have further curtailed the theory by neglecting the dependence of V^s on $\vec{q}$,

$$V^s(\vec{p},\vec{p}',\vec{q})=V_0^s=2v_0 \text{ (a constant)} , \tag{13}$$

and we have three parameters to determine: ϵ_0, M, and V_0^s. In this simple case we obtain the following expressions for the chemical potential, the surface tension, and the surface density of normal fluid.

Chemical potential:

$$\mu_3=-\epsilon_0+\tfrac{1}{2}N_sV_0^s+k_BT\ln\eta , \tag{14}$$

where $\eta=e^{T_{FS}/T}-1$ and the surface Fermi energy $k_BT_{FS}=\pi\hbar^2N_s/M$.

Surface tension:

$$\Delta\sigma\equiv\sigma(T)-\sigma_4(0)=-aT^{7/3}-\frac{M}{\pi\hbar^2}(k_BT)^2S_1(\eta)-\tfrac{1}{4}N_s^2V_0^s , \tag{15}$$

where

$$S_1(\eta)=\begin{cases}\dfrac{\pi^2}{6}+\tfrac{1}{2}(\ln\eta)^2+\displaystyle\sum_{m=1}^{\infty}\frac{(-1)^m}{m^2}\eta^{-m} & \text{when } \eta\geq 1 ,\\ -\displaystyle\sum_{m=1}^{\infty}\frac{(-1)^m}{m^2}\eta^m & \text{when } \eta\leq 1 ,\end{cases} \tag{16}$$

and the ripplon contribution to $\Delta\sigma$ is

$$\Delta\sigma_4=-aT^{7/3}=-0.1340(\rho_0/\sigma_0\hbar^2)^{2/3}(k_BT)^{7/3}=-(6.50\times10^{-3})T^{7/3}\ \text{erg cm}^{-2} . \tag{17}$$

Normal-fluid density[4]:

$$\nu_n=N_sM+bT^{5/3} , \tag{18}$$

where the ripplon contribution to the normal-fluid density is

$$\nu_4=bT^{5/3}=5(k_BT)^{5/3}[\rho\hbar/\sigma_4(0)]^{4/3}\Gamma(\tfrac{5}{3})\zeta(\tfrac{5}{3})/18\pi\hbar^2=(1.68\times10^{-10})T^{5/3}\ \text{g cm}^{-2} . \tag{19}$$

Using Eqs. (12), (14), and (15) the surface entropy density is the same as that of an ideal two-dimensional gas:

$$S=\tfrac{7}{3}aT^{4/3}+\frac{M}{\pi\hbar^2}(k_B^2T)[2S_1(\eta)-\ln(1+\eta)\ln\eta] . \tag{20}$$

If we neglect the ripplon contribution to the entropy and the surface tension, since

$$N_s=\frac{M}{\pi\hbar^2}k_BT_{FS}=\frac{M}{\pi\hbar^2}k_BT\ln(1+\eta) , \tag{21}$$

the entropy per particle S/N_s is a function of η alone. In this case

$$-\nu_nu_s^2=\left(\frac{\partial\Delta\sigma}{\partial\ln N_s}\right)_\eta=\left(\frac{\partial\Delta\sigma}{\partial\ln T}\right)_\eta=2\Delta\sigma ,$$

so that

$$u_s^2=-2\Delta\sigma/N_sM . \tag{22}$$

The rather complicated formula which results when the ripplon contributions to $\Delta\sigma$ and ν_n are not neglected has also been derived. Although we used the complicated formula in the computer program to be described in Sec. IV B, at 100 mK it makes a difference of only 0.1 m/sec in u_s for the concentrations that are represented in Fig. 8. This is only one-fifth of the standard deviation of our data.

B. Fitting the data

We have made a least-squares fit to our 91 measurements of $\Delta\sigma$ and 37 measurements of u_s with the theory outlined in Sec. IV A, assuming that $V^s(\vec{p},\vec{p}',\vec{q})$ can be approximated by a constant V_0^s, i.e., a δ-function interaction in real space. The equations fitted are (14), (15), and (22) supplemented by the fact that the chemical potential in the interior of the liquid is the same as that on the surface:

$$\mu_3=k_BT\ln[\tfrac{1}{2}n_3(2\pi\hbar^2/mk_BT)^{3/2}] . \tag{23}$$

Here n_3 and m are the number density and effective mass in the interior, and the total number of ^{3}He is conserved for each sample:

$$N_s+n_3(V/A)=N_{si}^0 , \tag{24}$$

where N_{si}^0 is the value of N_s on the ith sample at 0 K, and V/A is the ratio of volume to area. In using Eq. (24) the value of m, the effective mass in the interior, was taken to be $2.28m_3$ (Ref. 19). The standard deviation for the surface-tension data was taken to be 3.78×10^{-5} erg cm^{-2} and for the velocity of surface sound 0.5 m/sec. In making the fit there are five adjustable constants: ϵ_0, M, V_0^s, and the experimental parameters V/A and N_{s1}^0, the amount of ^{3}He on the surface of the first sample. (The amount of ^{3}He added to obtain the second sample

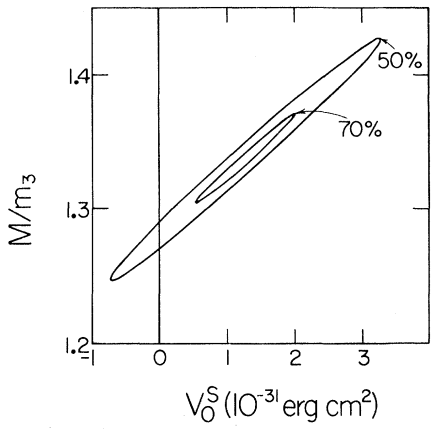

FIG. 10. Fit to the present surface-tension and surface sound data in the V_0^s, M/m_3 plane. The contours give the χ^2 probability i.e., the probability that the deviations are just due to experimental error.

was accurately known.)

The results of the fit are given in Fig. 10, which shows contours of constant χ^2 as a function of V_0^s and M. This graph was generated by holding V_0^s and M at various fixed values and adjusting the other three parameters to their optimum values. The percentages on the contours are values of the "χ^2 probability," which is the probability that the experimental deviations from the theory are due to chance and not to any inadequacy in the theory or in an assumed value of a parameter. The fit at the center of the contours is quite satisfactory, corresponding to a probability larger than 70%. Even if we put $V_0^s=0$, which corresponds to an ideal gas, the fit is still acceptable, so that an ideal-gas model is certainly consistent with all of our data. This fit, which has $M=1.28m_3$ and $\epsilon_0/k_B=2.28$ K, is shown as the full curves in Figs. 8 and 9. With regard to the effective interaction we can conclude only that V_0^s is in the range -1×10^{-31} to 3×10^{-31} erg cm^2, which means that the interaction is probably repulsive, corresponding to a positive value of V_0^s.

The optimum values for the binding energy ϵ_0/k_B which go with the fits represented in Fig. 10 vary very little, by not more than 10 mK for all fits with acceptable χ^2 probabilities, so that an important part of the uncertainty in ϵ_0 comes from the uncertainty in our temperature scale. We conclude on this basis and in agreement with the other fits described below, that ϵ_0 is given by

$$\epsilon_0/k_B=2.28\pm0.03\ \text{K}.$$

The values of ϵ_0 and M obtained above are rather different from the results quoted by Guo *et al.*,[3] which were obtained from surface-tension measurements on samples of considerably higher ^{3}He concentration than in the present work. They gave $\epsilon_0/k_B=1.95\pm0.1$ K, $M/m_3=1.7\pm0.3$, and $V_0^s=(-1.5\pm1.3)\times10^{-31}$ erg cm^2. This discrepancy is not due to any disagreement in the data (see below), it is due to the method of extrapolation to zero concentration which was used by Guo *et al.* They noticed that a graph of $\Delta\sigma^{1/2}$ versus μ_3 at $T=0$ based on their data could be represented by a hyperbola, and used this fact to extrapolate the graph to zero concentration to obtain a value of ϵ_0. The hyperbola leads to an ϵ_0 which is too low and a slope which is too high, giving rise to a negative V_0^s.

We have shown that the present measurements and the data of Guo *et al.* are completely consistent by making a combined fit of their data and ours to the theoretical model. We also have included some unpublished surface-tension data of Crum[22] on samples of a few hundred ppm which agree with those of Guo *et al.* We used 32 data points of Guo *et al.* and Crum, all those with surface concentrations below 5×10^{14} cm^{-2}, with the quoted standard deviation of 0.003 erg cm^{-2}. The results are given in Fig. 11, which is a plot similar to that in Fig. 10. The agreement with the theory is improved and the uncertainty in M and V_0^s is reduced considerably. The values of ϵ_0 are not appreciably changed from those in the previous fit.

Before drawing our final conclusions about the values of M and V_0^s we ought to remark that the uncertainty in these parameters depends on the complexity of the model chosen to represent the data. If the higher-order terms in the interaction, determined by the parameters v_1 and v_2, and the $\gamma p^4/2M$ term in the quasiparticle spectrum are not put equal to zero, the number of adjustable parameters in the fit is increased by three. The χ^2 probabilities would then be increased but the allowed latitude in M and V_0^s would also be increased. Unfortunately the formula for u_s as a function of N_s and T in this

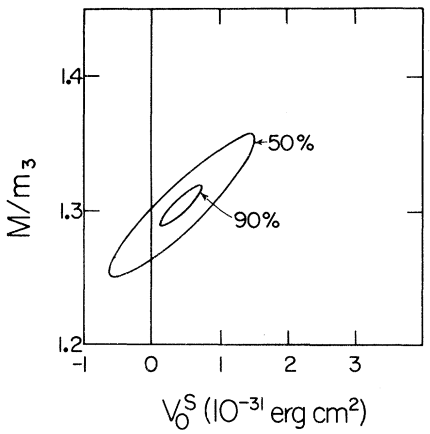

FIG. 11. Same as in Fig. 10, except that the low-density surface-tension measurements of Guo *et al.* (Ref. 3) and Crum (Ref. 22) have been added to the data.

case seemed too complicated for us to derive conveniently although the result for $T=0$ was obtained. We could then only make a fit using extrapolations of the u_s data to $T=0$ for our two samples. Such a fit does not pin down the parameters as well as a fit at finite temperature. The results of this somewhat unsatisfactory procedure were as expected. No significant conclusions could be drawn as to the sign of v_1, v_2, or γ; ϵ_0 was not significantly changed; the values of M fell in the range $M/m_3 = 1.45 \pm 0.1$; V_0^s was between 0 and 3×10^{-31} erg cm^2. Further progress could probably be made in this direction if we had data on a larger range of sample concentrations, as well as the equation for u_s at finite temperature.

On the basis of Fig. 11 one might conclude that $M/m_3 = 1.30 \pm 0.05$ and $V_0^s = (0.5 \pm 1.0)\times10^{-31}$ erg cm^2; however in view of the danger of unsuspected systematic errors and the discussion in the preceding paragraph we deduce that $M/m_3 = 1.3 \pm 0.1$ and that $V_0^s = (0.5 \pm 2.0)\times10^{-31}$ erg cm^2 are reasonable conclusions from the data. These limits on V_0^s show it to be very weak. It is customary to compare V_0, the corresponding quantity in three dimensions, to $m_4 s^2/n_4$, where s and n_4 are the velocity of sound and number density in pure ^{4}He. This gives $V_0 \simeq 0.08 m_4 s^2/n_4$. In comparison the corresponding quantity for the surface $0.08 m_4 s^2/(n_4)^{2/3} = 8\times10^{-31}$ erg cm^2, an order of magnitude larger than the value from Fig. 11.

C. Mechanism for surface-sound generation and detection

As we described in Sec. III A, surface sound was generated by a short (~20-μsec) pulse of heat applied to a graphite film resistor partially immersed in the liquid, and detected by a similar resistor used as a bolometer. The observation shown in Fig. 7, that the amplitude of the signal is proportional to the length of the transmitter above the liquid meniscus, demonstrates that the saturated helium film on the upper part of the resistor is important in converting the heat pulse into surface sound. The signal also depends on the exposed area of the receiver so that the helium film probably plays a part in the detection of the sound as well.

In some thermal-analysis measurements[10] that we have carried out on similar graphite resistors it was found that, although the heat capacity of the graphite itself is negligibly small, the heat capacity of the plastic backing is comparable with or larger than the heat capacity of the ^{3}He-^{4}He film. Moreover the Kapitza conductance from the graphite to the backing is approximately an order of magnitude larger than that to the helium. During the short but intense heat pulse, the graphite rises to a temperature of between 0.6 and 1 K (depending on the heating power), which is much higher than that of the backing or the helium film. The heat then divides itself between the helium and the backing according to the Kapitza conductances. To fit the experimental results (shown in Fig. 12) we have had to assume that $\frac{1}{4}$ of the heat input to the transmitter reached the helium film. (Compare the upper horizontal scale, which is the heat input per unit area q with the lower scale which is the heat reaching the ^{3}He-^{4}He film.)

Since the helium film is heated so rapidly it is reasonable to assume that the amount of ^{3}He covering its surface (N_s) plus the amount dissolved in the interior of the film ($N_s^0 - N_s$) remains constant during the heating pulse and that the expansion of the surface ^{3}He "gas" which generates the sound takes place relatively slowly. With this assumption it is easy to calculate the change in the surface tension of the film $\sigma^0 - \sigma$ due to the increase in its energy per unit area, $U - U^0$:

$$U - U^0 = (\Delta\sigma_3^0 - \Delta\sigma_3) + \tfrac{4}{3}(\Delta\sigma_4^0 - \Delta\sigma_4) + (N_s^0 - N_s)(\tfrac{3}{2}k_B T + \epsilon_0)\,. \tag{25}$$

Here we have used the fact that, as in a two-dimensional ideal gas, the kinetic-energy density of the surface ^{3}He is equal to the negative of its contribution to the surface tension, $-\Delta\sigma_3(N_s, T)$, and that the ripplon energy is $-\frac{4}{3}\Delta\sigma_4(T)$. We have included in the energy U the contribution from the dissolved ^{3}He, the term in $N_s^0 - N_s$. Now $\Delta\sigma_3$ and $\Delta\sigma_4$ are known functions of N_s and T, and N_s can be calculated from T using the equilibrium condition between dissolved ^{3}He and surface ^{3}He. Therefore Eq. (25) can be solved to find $\sigma^0 - \sigma$ as a function of $U - U_0$. The results, calculated for our first sample, $N_s^0 = 0.97\times10^{14}$ cm^{-2}, starting at $T^0 = 0.03$ K and assuming a film thickness of 300 Å are shown in Fig. 12. At point A on the curve ^{3}He begins to dissolve in the film. At B two things occur: First, the surface-tension change $\sigma^0 - \sigma$ reaches saturation. This is because the decrease in the magnitude of $\Delta\sigma_3$ due to ^{3}He dissolving in the film is balanced by the increase in the ripplon contribution $\Delta\sigma_4$. Second, appreciable ^{3}He evaporation begins at this temperature, reducing any further increase in the temperature with the applied heat. It appears that the shape of the theoretical curve for $\sigma^0 - \sigma$ approximates the observed signal amplitude versus heat input, shown as circles, so that we are able to understand why the signal amplitude saturates at a q of about 17 merg cm^{-2}. We note that, at saturation, the temperature of the helium film has reached 0.3 K. Since this is much higher than the ambient temperature of a typical experiment, say 0.03 K, one might expect to generate a "shock" wave instead of the desired "small-amplitude" surface-sound wave. As was shown in Sec. III A, there was no observed dependence of the sound velocity on signal amplitude so presumably the shock effect dissipates itself suf-

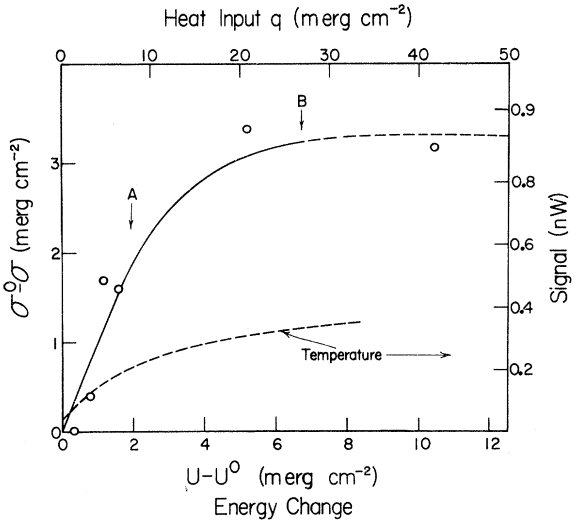

FIG. 12. Full line represents the theoretical relation between the decrease in surface tension $\sigma^0 - \sigma$ and the energy change $U - U^0$ in the film covering the transmitter, calculated from Eq. (25). The dashed curve gives the temperature of the film (right-hand ordinate). The circles are measurements of the surface-sound signal (right-hand axis) versus the heat input q adjusted to roughly fit the theory. The theory explains the saturation in the signal which occurs beyond $q = 10$ merg cm^{-2}.

ficiently fast that it has a negligible effect over the majority of the flight path.

As observed at the receiver the signal usually appeared as a "heating" followed by a similar "cooling" (see Figs. 2, 3, and 7). The energy involved in each of these two halves of the signal, about 10^{-6} erg, is much smaller than the energy put into the surface at the receiver, about 2×10^{-3} erg cm^{-2}. Allowing for the spreading of the signal from the transmitter one would expect to see about 5×10^{-5} erg at the receiver. The discrepancy is perhaps due to the large Kapitza resistance between the receiver and the helium film.

The characteristic heating then cooling form of the signal is quite hard to explain since the separation of these two parts of the signal did not depend on the length of the heating pulse. However, it did depend on the height of the film-covered part of the receiver. To understand this we attempted to correct for the effect of the finite size of the saturated film on the detector. It is obvious that since the surface sound travels over the film covering the detector in a finite time the signal that the detector sees is a space-averaged version rather than one seen by a point observer. The point-observer signal can be reconstructed by writing down difference equations relating the averaged signals at different flight times to a nonaveraged signal at one particular flight time. The reconstruction shows that the corrected point-observer heating and cooling pulses have lengths that are independent of the size of the receiver and each equal to 130 μsec for the first helium sample. This result was obtained at several temperatures and for different heater sizes provided the heat input was not large enough to produce appreciable evaporation. The analysis was not carried out so extensively for the second sample but it appears that the signal length was roughly the same. At present we cannot account for this characteristic time of 130 μsec which corresponds, when multiplied by the surface-sound velocity, to a length of about 4 mm. It did not vary with the height of the film on the transmitter.

V. CONCLUSIONS

The analysis of our data shows that the effective quasiparticle interaction is so weak as to have little measurable effect on the thermodynamic and hydrodynamic properties of surface ^{3}He at low densities. Recently the theory[23] of the transport coefficients for surface ^{3}He has been published. The diffusion coefficient, viscosity, and thermal conductivity are expressed in terms of the effective quasiparticle interaction and numerical estimates of their magnitude were obtained using our value of V_0^s. The experimental measurement of these quantities would be very useful in determining the interaction accurately. The very small, positive value of V_0^s which we have obtained indicates a predominantly repulsive interaction at large distances, which is unfortunately unfavorable for the observation of two-dimensional superfluidity. However, the effect of higher-order terms in the interaction remains open and further measurements where the surface density N_s approaches a monolayer or more may prove interesting in this regard.

The binding energy ϵ_0 is the best determined quantity in our experiment, since it does not depend on the choice of the theoretical model for surface ^{3}He. In fact, the largest uncertainty in our value $\epsilon_0/k_B = 2.28 \pm 0.03$ K is associated with the temperature measurement. Several theoretical calculations have been performed in the past few years to predict the value of ϵ_0. Saam[24] gave $\epsilon_0/k_B = 1.26$ K and Shih and Woo[25] estimated $\epsilon_0/k_B = 1.6$ K. Our experimental value agrees rather well with a recent calculation by Chang and Cohen,[26] who found $\epsilon_0/k_B = 2.35$ K. At present there are no published calculations of the effective mass M. The fact that M is close to the mass of a ^{4}He atom and that the quasiparticle interaction is so weak may suggest new theoretical ideas on this subject.

As we pointed out in Sec. III A, our data on the surface sound velocity do not agree with Eq. (2) in the region where ^{3}He begins to dissolve into the bulk. We regard this result to be due to coupling between the bulk excitations and the surface excitations. Below about 90 mK, the theory underlying

Eq. (2) for the surface-sound velocity is confirmed very effectively.

Andreev and Kompaneets have proposed[27] that there should be a first-order phase transition on the free surface of a ^{3}He solution due to condensation of the surface ^{3}He into a two-dimensional liquid. The transition would be accompanied by a change in slope of the temperature plot of the surface tension. They also estimated the surface density of the supposed liquid to be $N_s = 2\times10^{15}$ cm^{-2}. After correcting for an error of a factor of 10 that Andreev and Kompaneets made in reading the surface tension from a graph in Guo *et al.*,[3] their estimate should be 2×10^{14} cm^{-2}. We have used the data of Guo *et al.* together with that of Crum[22] in a similar way and find that the density of the supposed liquid cannot be larger than 1.3×10^{14} cm^{-2} at 0 K. This density corresponds to about $\frac{1}{4}$ of an atomic layer and it seems rather small for a liquid phase. As we have seen, the almost ideal-Fermi-gas model accounts for our observations of the surface tension and the surface sound very well. We therefore see no evidence for the proposed liquid-gas transition at the present time.

ACKNOWLEDGMENTS

We would like to thank Professor C. Ebner and Professor W. F. Saam for many stimulating and interesting discussions concerning the surface properties of liquid helium, and R. L. Kindler for his meticulous work on the experimental apparatus.

APPENDIX

In this appendix we obtain expressions for the surface tension and some other thermodynamic properties of the surface and for the velocity of surface sound u_s assuming the interacting quasiparticle model described in Sec. IV A of the text. The formulas are closely parallel to similar ones in three dimensions for bulk ^{3}He quasiparticles.[19,20]

Although the surface tension is the surface density of the "canonical" free energy, whose conjugate variables are μ_3 and T, in practice it is more convenient to obtain $\Delta\sigma_3$, μ_3, and the normal-fluid density in terms of the variables N_s and T.

Following the procedure used by Disatnik and Brucker in three dimensions, we write the energy per unit area of the surface, given by Eq. (5), in terms of the interaction $U(\vec{p}, \vec{p}')$ averaged over spin:

$$U^s = U_4^s + \int(2d\tau)\epsilon(\vec{p})n(\vec{p}) + \frac{1}{2}\int(2d\tau)(2d\tau')U(\vec{p}, \vec{p}')n(\vec{p})n(\vec{p}'), \tag{A1}$$

where $d\tau = d^2p/h^2$, $U(\vec{p}, \vec{p}')$ is given by Eq. (10),

$$U(\vec{p}, \vec{p}') = v_0 + v_1(\vec{p} - \vec{p}')^2 + v_2\vec{p}\cdot\vec{p}', \tag{10}$$

and

$$\epsilon(\vec{p}) = -\epsilon_0 + p^2/2M + \gamma(p^4/2M). \tag{4}$$

The number density N_s is

$$N_s = \int 2d\tau\, n(\vec{p}), \tag{A2}$$

and in the absence of surface currents,

$$\int 2d\tau\, n(\vec{p})\vec{p} = 0.$$

Substituting in Eq. (A1),

$$U^s = U_4^s - N_s\epsilon_0 + \tfrac{1}{2}N_s^2v_0 + \int 2d\tau\, n(\vec{p})(p^2/2M^*) + \gamma\int 2d\tau\, n(\vec{p})(p^4/2M), \tag{A3}$$

where

$$1/M^* = 1/M + 2v_1N_s. \tag{A4}$$

Using the fact that $dU^s = T\,dS + \mu_3\,dN_s$ and

$$S = -k_B\int 2d\tau\{[1-n(\vec{p})]\ln[1-n(\vec{p})] + n(\vec{p})\ln n(\vec{p})\}, \tag{A5}$$

we obtain

$$n(\vec{p}) = (e^{[e(\vec{p})-\mu_3]/k_BT} + 1)^{-1}, \tag{A6}$$

where

$$e(\vec{p}) = -\epsilon_0 + N_sv_0 + p^2/2M^* + \gamma(p^4/2M) + 2v_1M^*\int 2d\tau' n(\vec{p}')(p'^2/2M^*). \tag{A7}$$

Apart from the terms in γ, which we shall consider later, Eqs. (A2), (A3), and (A7) can be integrated to first order to give

$$U^s = U_4^s - N_s\epsilon_0 + \tfrac{1}{2}N_s^2v_0 + U_F^*, \tag{A8}$$

$$\mu_3 = \mu_F^* - \epsilon_0 + N_sv_0 + 2M^*v_1U_F^*, \tag{A9}$$

$$S = S_F^*, \tag{A10}$$

where $U_F^*(N_s, T)$, $\mu_F^*(N_s, T)$, and $S_F^*(N_s, T)$ are the energy per unit area, chemical potential, and entropy per unit area of an *ideal* two-dimensional gas of number density N_s and effective mass M^*. Since the ^{3}He contribution to the surface tension is the quasiparticle canonical free energy density,

$$\begin{aligned}\Delta\sigma_3 &\equiv \sigma(T, N_s) - \sigma_4(T)\\ &= (U^s - U_4^s) - TS - N_s\mu_3\\ &= -U_F^* - \tfrac{1}{2}N_s^2v_0 - 2M^*N_sv_1U_F^*.\end{aligned} \tag{A11}$$

The properties of the ideal gas, U_F^*, μ_F^*, etc., can be obtained from the canonical free energy of the ideal two-dimensional gas:

$$\sigma_F^* = -U_F^* = -k_BT\frac{4\pi M^*}{h^2}\int_0^\infty d\epsilon\ln(1+e^{-(\epsilon-\mu_F^*)/k_BT}) = -\frac{M^*}{\pi\hbar^2}(k_BT)^2S_1(\eta), \tag{A12}$$

where $\eta = e^{\mu_F^*/k_BT}$ and

$$S_1(\eta) = \int_0^\infty dx \ln(1+\eta e^{-x}) = \begin{cases} \frac{1}{2}(\ln\eta)^2 + \frac{1}{6}\pi^2 + \sum_1^\infty \frac{(-1)^m}{m^2}\eta^{-m} & \text{when } \eta \geq 1 \\ -\sum_1^\infty \frac{(-1)^m}{m^2}\eta^m & \text{when } \eta \leq 1 \ . \end{cases} \quad \text{(A13)}$$

From $N_s = -(\partial\sigma_F^*/\partial\mu_F^*)_T$ we obtain

$$N_s = \frac{M^*}{\pi\hbar^2}(k_BT)\ln(1+\eta)$$

and

$$\mu_F^* = k_BT\ln\eta = k_BT\ln(e^{\pi\hbar^2 N_s/M^*k_BT} - 1) \ , \quad \text{(A14)}$$

$$\eta = e^{\pi\hbar^2 N_s/M^*k_BT} - 1 \ . \quad \text{(A15)}$$

We now consider the effect of the term $\gamma p^4/2M$ ($\equiv \gamma^* p^4/2M^*$) in the quasiparticle energy. First we evaluate the change $\mu_F^{*\gamma}$ in the chemical potential of the ideal two-dimensional gas due to this term. We have

$$N_s = \frac{4\pi M^*}{h^2}\int_0^\infty d\epsilon\,(e^{\beta(\epsilon-\mu_F^*)}+1)^{-1} = \frac{4\pi M^*}{h^2}\int_0^\infty d\epsilon\,(e^{\beta(\epsilon+2M^*\gamma^*\epsilon^2-\mu_F^*-\mu_F^{*\gamma})}+1)^{-1} \ ,$$

where $\beta = 1/k_BT$. To first order in γ^*, this yields

$$\mu_F^{*\gamma} = 4\pi\hbar^2\gamma^*(1+e^{-\mu_F^*/k_BT})U_F^* = 4M^*\gamma^*(k_BT)^2(\eta+1)S_1(\eta)/\eta \ . \quad \text{(A16)}$$

The change in the ideal two-dimensional-gas canonical free energy $\sigma_F^{*\gamma}$ is determined from

$$\sigma_F^{*\gamma} = -k_BT\frac{4\pi M^*}{h^2}\int_0^\infty d\epsilon\,[\ln(1+e^{-\beta(\epsilon+2M^*\gamma^*\epsilon^2-\mu_F^*-\mu_F^{*\gamma})}) - \ln(1+e^{-\beta(\epsilon-\mu_F^*)})] \ .$$

To first order in γ^*

$$\sigma_F^{*\gamma} = -N_s\mu_F^{*\gamma} + 4M^{*2}\gamma^*(k_BT)^3S_2(\eta)/\pi\hbar^2 \ , \quad \text{(A17)}$$

where

$$S_2(\eta) = \int_0^\infty x\,dn\ln(1+\eta e^{-x}) = \begin{cases} \frac{1}{6}(\ln\eta)^3 + \frac{1}{6}\pi^2(\ln\eta) - \sum_1^\infty \frac{(-1)^m}{m^3}\eta^{-m} & \text{when } \eta \geq 1 \\ -\sum_1^\infty \frac{(-1)^m}{m^3}\eta^m & \text{when } \eta \leq 1 \ . \end{cases} \quad \text{(A18)}$$

Our final results are, combining (A11), (A12), (A15), (A16), and (A17),

$$\Delta\sigma_3(N_s, T) = -\tfrac{1}{2}N_s^2v_0 - \frac{M^*}{\pi\hbar^2}(k_BT)^2 \times \left[S_1(\eta)\left(1 + 2M^*N_sv_1 + 4\pi\hbar^2N_s\gamma^*\frac{1+\eta}{\eta}\right) - 4M^*\gamma^*(k_BT)S_2(\eta)\right] \ , \quad \text{(A19)}$$

and, from (A9), (A14), and (A16),

$$\mu_3(N_s, T) = -\epsilon_0 + N_sv_0 + k_BT\left[\ln\eta + 2M^*(k_BT) \times \left(\frac{M^*v_1}{\pi\hbar^2} + 2\gamma^*\frac{1+\eta}{\eta}\right)S_1(\eta)\right] \ , \quad \text{(A20)}$$

where

$$\eta = e^{\pi\hbar^2N_s/M^*k_BT} - 1 \quad \text{(A15)}$$

and

$$M^{*-1} = M^{-1} + 2v_1N_s \ . \quad \text{(A4)}$$

The above equations are sufficient to determine all of the thermodynamic properties of the surface ^{3}He. To obtain the velocity of surface sound we also need the normal-fluid density ν_n. We shall not discuss the calculation but simply state the result, valid to first order in γ and the interaction, which is analogous to the formula in three dimensions[19,20]:

$$\nu_n = N_sM\left(1 - \frac{8\gamma M^2}{\pi\hbar^2N_s}(k_BT)^2S_1(\eta) - N_sMv_2\right) \ . \quad \text{(A21)}$$

---

†Work supported by a grant from the National Science Foundation, GH 31650 A No. 2. The Ph.D. dissertation of S. Y. Shen was presented on this subject at the Ohio State University.

*Present address: Northwestern University, Evanston, Ill. 60201.

‡Present address: Logicon Inc., Los Angeles, Calif. 90733.

§Present address: State University of New York, Buffalo, N. Y. 14214.

[1] A. F. Andreev, Zh. Eksp. Teor. Fiz. 50, 1415 (1966) [Sov. Phys.-JETP 23, 939 (1966)].

[2] In this paper all ^{3}He chemical potentials and energies are measured with respect to the ground state of one ^{3}He atom in bulk ^{4}He. See Guo *et al.* (Ref. 3).

[3] H. M. Guo, D. O. Edwards, R. E. Sarwinski, and J. T. Tough, Phys. Rev. Lett. 27, 1259 (1971).

[4] A. F. Andreev and D. A. Kompaneets, Zh. Eksp. Teor. Fiz. 61, 2459 (1971) [Sov. Phys.-JETP 34, 1316 (1972)].

[5] J. R. Eckardt, D. O. Edwards, P. P. Fatouros, F. M. Gasparini, and S. Y. Shen, Phys. Rev. Lett. 32, 706 (1974).

[6] We are grateful to Dr. B. M. Abraham of Argonne National Laboratory for the generous gift of this thermometer.

[7] Cryocal, Inc., Riviera Beach, Fla. 33404.

[8] J. R. Eckardt, D. O. Edwards, F. M. Gasparini, and S. Y. Shen, *Low Temperature Physics-LT-13*, edited by K. D. Timmerhaus, W. J. O'Sullivan, and E. F. Hammel (Plenum, New York, 1974), Vol. 1, p. 518.

[9] D. O. Edwards, R. L. Kindler, and S. Y. Shen, Rev.

Sci. Instrum. (to be published).
[10]S. Y. Shen, Ph.D. dissertation (The Ohio State University, 1973) (unpublished).
[11]Biomation, 1070 E. Meadow Circle, Palo Alto, Calif. 94303.
[12]Nicolet Instrument Corp., 5225 Verona Road, Madison, Wisc. 53711.
[13]F. M. Gasparini, J. R. Eckardt, D. O. Edwards, and S. Y. Shen, J. Low Temp. Phys. 13, 437 (1973).
[14]D. O. Edwards, J. R. Eckardt, and F. M. Gasparini, Phys. Rev. A 9, 2070 (1974).
[15]J. R. Eckardt, Ph.D. dissertation (The Ohio State University, 1973) (unpublished).
[16]D. O. Edwards, in Ref. 8, Vol. 1, p. 26.
[17]W. M. Whitney and C. E. Chase, Phys. Rev. 158, 200 (1967).
[18]K. R. Atkins, Can. J. Phys. 31, 1165 (1953).
[19]C. Ebner and D. O. Edwards, Phys. Rep. C 2, 77 (1971).
[20]Y. Disatnik and H. Brucker, J. Low Temp. Phys. 1, 491 (1972).
[21]J. Bardeen, G. Baym, and D. Pines, Phys. Rev. 156, 207 (1967).
[22]D. B. Crum, Ph.D. dissertation (The Ohio State University, 1973) (unpublished).
[23]H. H. Fu and C. Ebner, Phys. Rev. A 10, 338 (1974).
[24]W. F. Saam, Phys. Rev. A 4, 1278 (1971).
[25]Y. M. Shih and C.-W. Woo, Phys. Rev. Lett. 30, 478 (1973).
[26]C. C. Chang and M. Cohen, Phys. Rev. A 8, 3131 (1973).
[27]A. F. Andreev and D. A. Kompaneets, Zh. Eksp. Teor. Fiz. Pis'ma Red. 17, 379 (1973) [JETP Lett. 17, 268 (1973)].